RESPONSE TO REQUEST FOR ADDITIONAL INFORMATION

07/08/2013

US-APWR Design Certification

Mitsubishi Heavy Industries

Docket No. 52-021

RAI NO.:	**NO. 1023-7067 REVISION 3**
SRP SECTION:	**03.08.03 – Concrete and Steel Internal Structures of Steel or Concrete Containments**
APPLICATION SECTION:	**3.8.3**
DATE OF RAI ISSUE:	**04/26/2013**

QUESTION NO. 03.08.03-110:

The staff reviewed MUAP-11005-P, Revision 1, dated December 27, 2012. The staff found that the updated MUAP-11005, Revision 1 report incorporated the information presented in the response to RAI 958-6608, Question 03.08.03-93. The staff requests the following to be addressed:

1. On Page B-7, Figure B-2 shows a number of test data points that line up along a vertical line, which is indicative that the calculated shear strength values shown may only account for the concrete and do not include the contribution from the shear reinforcement. This is inconsistent with Table A-4-1 of MUAP-11013, Revision 2, in which the shear reinforcement contribution to the out-of-plane shear strength was taken into account. Although the shear reinforcement spacing (400 mm) is large in comparison with the steel concrete (SC) wall specimen depth (500 mm), the shear reinforcement may contribute to the out-of-plane shear strength if it crosses the diagonal cracking plane. Therefore, the staff requests that the applicant correct the inconsistency between the information provided in the two references cited and to consider the shear strength contribution from the shear reinforcement if it does contribute to the shear strength.

2. MUAP-11019, Revision 1, Section 7.2 discusses the tests reported by Sasaki et al. (1995) for SC wall in-plane shear capacity. Since this test was not discussed in MUAP-11005, Revision 1, which is intended to describe all testing related to SC design, the staff requests that the applicant include discussions on these tests. In addition, the paper by Sasaki et al. (1995) indicated that there were breaking and bond failures of studs. The staff requests that the applicant explain why stud failures occurred during the shear wall tests and how the failures can be avoided in US-APWR SC walls.

3. MUAP-11005, Revision 1, Page C-4, Figure C-2 appears to be the same as MUAP-11019, Revision 1, Figure 7.2-1. However, MUAP-11005, Revision 1, Figure C-2 shows that one test point is on the diagonal line, which means that the calculated value is equal to the experimental value; but MUAP-11019, Revision 1, Figure 7.2-1 shows the corresponding test point is below the diagonal line, which means that the calculated value is lower than the

experimental value. The staff requests that the applicant to correct the inconsistency between the calculated value and the experimental value shown in the figures.

4. MUAP-11005, Revision 1, Page C-6, Equation C-1, the ACI 349-06 equation quoted for in-plane shear strength design of RC walls is different by making comparison presented in MUAP 11005, Revision 1, based on the in plane shear strength equation and equation presented in MUAP-11019, Revision 1, Section 7.1. The staff requests that the applicant to correct the inconsistency; otherwise, provide the technical basis for Equation C-1.

5. Correct the following inconsistencies, missing information, and typos in MUAP-11005, Revision 1:

a) Page B-3, Table B-2, the top of the table was cutoff.

b) Page B-5, first and last paragraphs, the value ranges of Sstud/tp (stud spacing to faceplate thickness ratio, i.e., 22 to 44 and 20.8 to 30) are not consistent with the values in Table B-1 on Page B-2 (which shows 15 to 30).

c) Page B-6, Figure B-1, the number of specimens from the test reported by Kanchi et al. (1996) is less than those listed in Table B-1 on page B-2. The staff requests that the applicant correct the inconsistency; otherwise, provide an explanation for the inconsistency.

d) Page B-8, the second paragraph from the bottom, first sentence, "SP1-4, and SP1-4", the second "SP1-4" should be "SP1-5".

e) Page C-5, Table C-2 indicates that the No.1 test specimen by Fujita et al. (1998) experienced a shear failure. It appears that the corresponding test report (Reference 11 of the MUAP report) indicated a flexural failure.

f) Page C-7, the last paragraph, "Equation C-" should be "Equation C-1". There are two locations to be corrected. Also, in this paragraph, the reference to MUAP-11019 Section 6.3 for in-plane shear strength equation appears to be inconsistent with the content of MUAP-11019 Section 6.3, which addresses out-of-plane shear strength.

g) Page D-1, 5th paragraph, "Specimens N20, N30, N40 and N50..." should be "Specimens NS20, NS30, NS40 and NS50..."

h) Page D-3, Table D-1, tests reported by Kanchi Masaki et al. (1996) and Sekimoto Hisashi et al. (1996), the cells for Loading Type and Failure Mode indicate "Not available (awaiting English translation)". These cells should be updated, since the English versions of the two papers are included in MUAP-11005, Revision 1. Also in the table, tests reported by Kanchi Masaki et al. (1996), some values of Sstud/tp (stud spacing to faceplate thickness ratio) appear to be inconsistent with the test report.

i) Page D-4, Figure D-2, two specimens from the test reported by Usami et al. (1995) seem to have identical Sstud/tp (stud spacing to faceplate thickness ratio) values, which appears to be inconsistent with Table D-1. Also, the tests reported by Sekimoto Hisashi et al. (1996) are included in Table D-1, but not in Figure D-2. Furthermore, the tests reported by Akiyama et al. (1991) and Choi and Han (2009) are included in Figure D-2, but not in Table D-1, and the corresponding papers were not included in MUAP-11005, Revision 1.

ANSWER:

1. Technical Report MUAP-11019, Rev. 1 illustrates the portions of American Concrete Institute (ACI) 349-06 that are applicable to steel concrete (SC) design. Specifically, the report (a) identifies the equations in the ACI 349 code and appendices that are being used, (b) presents the technical bases for the use of the specified ACI code equations for SC walls, (c) and describes how the equations from the ACI code and provisions are to be utilized in the design of SC walls. Technical Report MUAP-11019, Rev. 1 does not explicitly call out all the code provisions that apply to SC design, but instead adopts the related provisions unless otherwise stated. In this case, only the out-of-plane shear strength formulations are given in Technical Report MUAP-11019, Rev. 1 for contributions coming from concrete and shear reinforcement. As stated in Technical Report MUAP-11019, Rev. 1, Section 2.6, the shear reinforcement spacing requirements given in Section 11.5 of ACI 349-06 apply to SC design. Section 11.5.5.1 of ACI 349-06 specifies that the shear reinforcement spacing limit to be d/2 for nonprestressed members. Since some of the specimens tested by Hong et al. (2011) exceeded the spacing limit (250mm), the shear strength contribution from shear reinforcement should not considered in the code design strength. Figure B-2 of Technical Report MUAP-11005, Rev. 1 has shown the comparison of the experimental strength with the calculated design strength based on accounting for the shear reinforcement spacing limits. The tabulated values for the MUAP design equation strength provided in Table A-4-1 of MUAP-11013, Rev. 2 will be revised to be consistent with Figure B-2 of Technical Report MUAP-11005, Rev. 1. These corrections improve the demonstrated conservatism of the design equations.

2. The Sasaki et al. reference paper will be added to Appendix E of Technical Report MUAP-11005, Rev. 1. The specimens tested will be added to Table C-2 of Technical Report MUAP-11005, Rev. 1. These tested specimens had an S_{stud} / t_p (stud spacing to faceplate thickness ratio, or steel plate slenderness ratio) of 33.0. This ratio is approximately twice the typical S_{stud} / t_p ratios used in US-APWR SC design as given in Table A-2 of Technical Report MUAP-11005, Rev. 1.

   The experimental behavior of the tested specimens stated in the Sasaki paper has indicated that all the specimens failed in plate buckling which occurred after yielding for all the specimens. It is also stated that the specimens were brought to the maximum load level without sudden load drops or slippage, which would be an indication of stud failure. Therefore, the stud failures have occurred after reaching the maximum load stage and the specimens have shown good ductility by maintaining 70 percent - 80 percent of the maximum load. As specified in Section 2.2 of Technical Report MUAP-11019, Rev. 1, the maximum permitted steel plate slenderness ratio (S_{stud} / t_p) for the US-APWR is 20. This limit eliminates the failure mode of local buckling before developing full compressive strength and no change to the design approach is required.

3. Figure C-2 of Technical Report MUAP-11005, Rev. 1 will be revised to be consistent with Figure 7.2-1 of Technical Report MUAP-11019, Rev. 1.

4. The in-plane shear strength design equation presented in Equation C-1 of Technical Report MUAP-11005, Rev. 1 will be revised to be identical to the equation given in Section 7.1 of Technical Report MUAP-11019, Rev. 1.

5. a) Table B-2 on Page B-3 of Technical Report MUAP-11005, Rev. 1 will be revised to resolve the formatting.

   b) The typographical errors on S_{stud} / t_p ratios given in Page B-5 of Technical Report MUAP-11005, Rev. 1 will be corrected to resolve the inconsistency.

c) All the specimens tested by Kanchi et al. (1996) are shown in Figure B-1 of Technical Report MUAP-11005, Rev. 1. However two specimens appear to be missing from the figure because of having almost identical experimental strength and MUAP design strengths to other two specimens. As it can be seen from the tabulated values given in Table A-4-1 of Technical Report MUAP-11013, Rev. 2, specimens #3 - #4 and #2 - #5 have very similar $V_{n\text{-}EXP}$ and $V_{n\text{-}FEM}$ values that result in these two specimen sets appearing as one data point for each set in the figure.

d) The typographical error will be corrected as noted.

e) The failure mode reported for Specimen No.1 given in Table C-2 of Technical Report MUAP-11005, Rev. 1 will be revised to flexural failure.

f) The typographical errors on equation numbering will be resolved. The typographical error in section numbers will be corrected to refer to Technical Report MUAP-11019, Rev. 1, Section 7.3.

g) The typographical errors in the specimen names will be resolved.

h) The cells in Table D-1 of Technical Report MUAP-11005, Rev. 1 will be updated to include the Loading Type and Failure mode of the specimens from the English translations. The S_{stud} / t_p ratios will be revised in Table D-1.

i) The data points shown in Figure D-2 for experiments conducted by Usami et al. (1995) appear to be inconsistent due to the figure providing buckling strength values for both sides of two of the four specimens. In other words, for this experimental program a total of six data points are shown for four specimens. (Two data points have similar values and are indistinguishable from each other in the figure.) The additional two data points result from reporting two buckling strengths for each faceplate of two of the specimens.

   All the test data available for compressive loading tests are provided in Figure D-2 of Technical Report MUAP-11005, Rev. 1. The test report by Sekimoto Hisashi et al. (1996) given in Table D-1 is referring to the identical test program described in Akiyama et al. (1991) in Figure D-2. For clarity, the figure legend will be revised to eliminate the inconsistency.

Impact on DCD

There is no impact on the DCD.

Impact on R-COLA

There is no impact on the R-COLA.

Impact on PRA

There is no impact on the PRA.

Impact on Technical/Topical Report

Technical Report MUAP-11005 and Technical Report MUAP-11013 will be revised as indicated on the attached markups.

This completes MHI's response to the NRC's question.

12. Kitano, T.; Akita, S., Nakazawa, M.; Fujino, Y.; Ohta, H.; Yamaguchi, T.; Nakayama, T.; "Experimental Study on a Concrete-filled Steel Structure Part 4: Shear Tests (Outline of the experimental program and the results)", Summaries of Technical Papers of Annual Meeting, Architectural Institute of Japan. B-2, pp. 1057-1058, 1997

13. Ozaki, M., Akita, S., Takeuchi, M.;et al, "Experimental Study on Steel-plate-reinforced Concrete Structure,
Part. 41 Heating Tests (Outline of Experimental Program and Results),
Part. 42 Heating Tests (Thermal Deformation Behavior),
Part. 43 Heating Tests (Mechanical Aspects of SC Panels after Heating)",
Summaries of Technical Papers of Annual Meeting, Architectural Institute of Japan, 2000, pp. 1127-1132

14. Usami, S.; Akiyama, H., Narikawa, M.; Hara, K.; Takeuchi, M.; and Sasaki, N.; "Study on a concrete filled steel structure for nuclear power plants (part 2). Compressive loading tests on wall members", SMiRT-13, Porto Alegre, Brazil, August, 1995

15. Kanchi, M.; et al, "Experimental Study on Concrete-filled Steel Structure: Part 2 Compressive Tests Characteristics Test (1)", Summaries of technical papers of Annual Meeting Architectural Institute of Japan. B-2, Structures II, Structural dynamics nuclear power plants 1996, 1071-1072, 1996-07-30

16. Sekimoto, H., "Experimental Study on Concrete Filled Steel Shear Wall: Part 1 Compression Test of Seismic Wall", Summaries of technical papers of Annual Meeting Architectural Institute of Japan. Structures II 1991, 1659-1660, 1991-08-01

17. Akita, S; Ozaki, M; "Earthquake-Resistant Design Recommendation for Building Using Steel Plate Reinforced Concrete Structure (Design Method of Earthquake-Resistant Wall)", Technical Report of Architectural Institute of Japan, Dec., 2001, No.14, pp123-128

18. Ozaki, M. et al, "Study on Steel Plate Reinforced Concrete Panels Subjected to Cyclic In-Plane Shear", Nuclear Engineering and Design, Volume 228, 2004

19. Varma, A.; Malushte, S.; Sener, K.; Both, P.; Coogler, K.; "Steel-Plate Composite (SC) Walls: Analysis and Design Including Thermal Effects", SMiRT 21, New Delhi, India, November 2011

(Part 2)

The full research reports of these references are provided in Appendix E.

20. Sasaki, N., Akiyama, H., Narikawa, M., Hara, K., Takeuchi, M., and Usami, S., "Study on A Concrete Filled Steel Structure for Nuclear Power Plants Part 3 Shear and Bending Loading Tests on Wall Member," 13th International Conference on Structural Mechanics in Reactor Technology, 1995.

[13] Ozaki, M., Akita, S., Takeuchi, M.;et al,"Experimental Study on Steel-plate-reinforced Concrete Structure Part. 41 Heating Tests (Outline of Experimental Program and Results), Part. 42 Heating Tests (Thermal Deformation Behavior), Part. 43 Heating Tests (Mechanical Aspects of SC Panels after Heating)", Summaries of Technical Papers of Annual Meeting, Architectural Institute of Japan, 2000, pp. 1131-1132

[14] Usami, S.; Akiyama, H., Narikawa, M.; Hara, K.; Takeuchi, M.; and Sasaki, N.; "Study on a concrete filled steel structure for nuclear power plants (part 2). Compressive loading tests on wall members", SMiRT-13, Porto Alegre, Brazil, August, 1995

[15] Kanchi, M.; et al, "Experimental Study on Concrete-filled Steel Structure: Part 2 Compressive Tests Characteristics Test (1)", Summaries of technical papers of Annual Meeting Architectural Institute of Japan. B-2, Structures II, Structural dynamics nuclear power plants 1996, 1071-1072, 1996-07-30

[16] Sekimoto, H., "Experimental Study on Concrete Filled Steel Shear Wall: Part 1 Compression Test of Seismic Wall", Summaries of technical papers of Annual Meeting Architectural Institute of Japan. Structures II 1991, 1659-1660, 1991-08-01

*The full research reports of these references are provided in Appendix E

(Part 2)

[20] Sasaki, N., Akiyama, H., Narikawa, M., Hara, K., Takeuchi, M., and Usami, S., "Study on A Concrete Filled Steel Structure for Nuclear Power Plants Part 3 Shear and Bending Loading Tests on Wall Member," 13th International Conference on Structural Mechanics in Reactor Technology, 1995.

Table B-2 Korean Out-of-Plane Shear Tests (Reference 2)

Replace table with 'Revised Table B-2' attached

Revised Table B-2

15 to 30

Japanese researchers have tested 16 SC beams that had combinations of shear studs and round tie bars anchored to concrete. Most of the specimens had shear span-to-depth ratios less than 1.5, with the exception of three specimens. The section depths were within the range from 8 in. to 24 in., or 203 mm to 609 mm. The steel faceplate reinforcement ratios varied from 1.33% to 4%, calculated based on the total steel area in the cross-section. The composite action factor (plate slenderness) which is defined as shear stud spacing to steel plate thickness (s_{stud}/t_p), varied from ~~22 to 44~~. The mechanical properties of steel and concrete used in these tests closely reflect the material properties that are specified in the actual design of US-APWR SC walls. Loading configurations ‘a’, ‘b’, and ‘c’ were used for testing the beams. The experimental program included 6 specimens (#8, #9, #10, S3, S4, S5, S6) having shear reinforcement out of total of 16 specimens. The geometric details for the specimens are given in Table B-1.

(Part 5b)

Specimen #7 had steel reinforcement ratios ($2t_p/T$) of 1.33%. This is within the range (1-2%) of the US-APWR Steel Reinforcement Ratio Category-1 (SRRC-1), and corresponds to US-APWR Section IDs 107 (refueling/reactor cavity walls) and 108 (north refueling cavity walls) as shown in Table A-2.

Specimens #2, #3, #4, #5, and #6 had steel reinforcement ratios ($2t_p/T$) of 2.0%. This is within the range (2-2.5%) of the US-APWR Steel Reinforcement Ratio Category-2 (SRRC-2), and corresponds to US-APWR Section IDs 103 (south reactor cavity walls) and 104 (secondary shield walls) as shown in Table A-2.

Specimens S1, S2, S3, S4, S5, and S6 had steel reinforcement ratios ($2t_p/T$) of 3.6%. This is within the range (3-4%) of the US-APWR Steel Reinforcement Ratio Category-4 (SRRC-4), and corresponds to US-APWR Section ID 105 (lower pressurizer walls) as shown in Table A-2.

Similarly, Specimens #1, #8, #9 and #10 had steel reinforcement ratios ($2t_p/T$) of 4.0%. This is within the range (4-5%) of the US-APWR Steel Reinforcement Ratio Category-5 (SRRC-5), and corresponds to US-APWR Section IDs 106 (mid-height pressurizer walls) as shown in Table A-2.

15 to 30

As indicated earlier, all 16 specimens had plate slenderness ratios (s/t_p), ranging from ~~20.8 to 30~~. This plate slenderness is larger than the s/t_p ratios (8 – 16) for US-APWR SC wall design for all Section IDs as shown in Table A-2. The specimens with shear reinforcement had similar shear reinforcement spacing to section depth ratios (s_{tie}/T). Specimens #9 and #10 had s_{tie}/T of 0.42 where the corresponding US-APWR Section 106 had 0.50. Furthermore, Specimens S3, S4, S5 and S6 had s_{tie}/T of 0.5 that is the identical ratio of the corresponding US-APWR section 105. Additionally, 10 of the specimens did not have any tie bars or connectivity between the two opposite steel faceplates.

(Part 5b)

strength calculated using TeR MUAP-11019 equations conservatively predicts the shear strengths for all the specimens. Only one specimen resulted in shear strength having same as the design equation; however this specimen failed in flexure before reaching its shear strength capacity.

Lastly, an experimental test program has been carried out at Purdue University, Bowen Laboratory particularly towards obtaining shear strength of unreinforced SC beams. The shear span to depth (a/d) ratio was kept in between 2.5 and 3.5. A total of five SC simply supported beams were tested. The specimens had only shear studs anchored to concrete but not any shear reinforcement. The geometric details for the specimens are given in Table B-3.

The specimens were designed so that in each specimen only one parameter was changed and keeping the rest unchanged from the reference specimen (SP1-1), to clearly observe its influence in the response. The parameters varied in this test group included the stud spacing (SP1-2), plate reinforcement ratio (SP1-3), shear span-to-depth ratio (SP1-4) and specimen scale ratio or depth (SP1-5). The scaled specimens were tested under three-point bending and the large-scale specimens were tested in four-point bending load configuration.

Specimen SP1-3 had a steel reinforcement ratio ($2t_p/T$) of 4.17%. This is within the range (4-4.5%) of the US-APWR SRRC 5, and corresponds to US-APWR Section IDs 106 (mid-height pressurizer walls) as shown in Table A-2. The plate slenderness ratio (s/t_p) for this specimen was twice of the corresponding US-APWR section, which was 16.0.

(Part 5d) Specimens SP1-1, SP1-2, SP1-4, and ~~SP1-4~~ SP1-5 had a steel reinforcement ratio ($2t_p/T$) of 2.78%. This is within the range (2.5-3%) of the US-APWR SRRC 3, and corresponds to US-APWR Section ID 101 (upper pressurizer wall) as shown in Table A-2. The plate slenderness ratios (s/t_p) for these specimens ranged from 20 to 48. This plate slenderness is larger than the corresponding s/t_p ratio (12) for US-APWR SC wall design for Section ID 101 as shown in Table A-2. Additionally, these specimens do not have any tie bars or connectivity between the two opposite steel faceplates.

Figure B-3 shows comparisons of the experimental results for the five specimens without shear reinforcement and compares them to the concrete shear strength contribution (V_c) calculated using Equations 6.2-1 of TeR MUAP-11019. The comparison indicates that the shear strength is conservatively estimated by the TeR MUAP-11019 design equation for all the specimens. The US-APWR SC walls have closely spaced rectangular tie bars. The behavior and ductility of the US-APWR SC walls will be better than those of the specimens that did not have any shear reinforcement. Nevertheless, the design strengths for out-of-plane shear can be estimated conservatively using TeR MUAP-11019 design equations.

Specimens S200NN, S300NN, and S400NN were subjected to pure in-plane shear (with zero axial compression). The tests were conducted cyclically, and the envelopes of the measured cyclic in-plane shear force-shear strain (V-γ) responses are shown in Figure C-1. The figure also includes comparisons with the predicted tri-linear in-plane shear force-shear strain responses for the specimens, the details of which were presented in Appendix A of TeR MUAP-11018. These comparisons were also shown in Appendix B of TeR MUAP-11018.

Section 4 of TeR MUAP-11018 explains how the initial, tangent, and secant stiffness calculated using the tri-linear in-plane shear force-shear strain response are used to define the stiffness of the cracked and uncracked SC walls of US-APWR Containment Internal Structure. Additional, numerical comparisons of the predicted and measured initial and post-cracking stiffness of these specimens are included in Appendix B of TeR MUAP-11018.

Figure C-2 shows additional comparisons of the experimental results for the seven specimens (S200NN, etc. as listed above) with those calculated using Equation 7.3-1 in TeR MUAP-11019. The comparison focuses on the in-plane shear strength (S_{xy}^{Y}) corresponding to Von Mises yielding of the steel faceplates. These comparisons were also included in Chapter 7 of TeR MUAP-11019. As shown, the TeR MUAP-11019 design equation conservatively predicts the in-plane shear strength of SC wall panels.

(Part 3)

Replace figure with 'Revised Figure C-2' attached

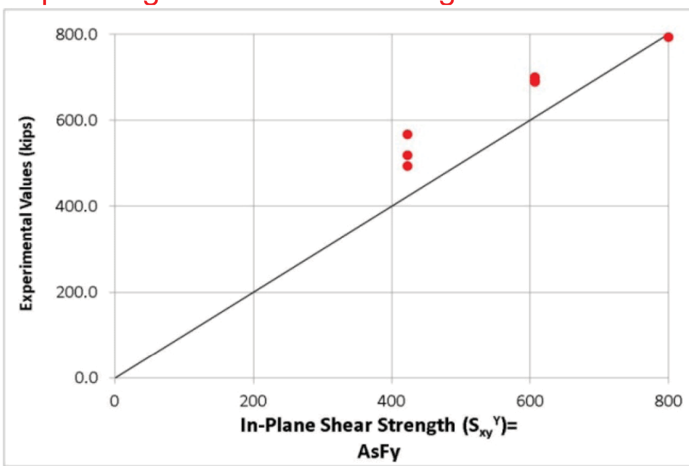

Figure C-2 Comparison of Experimental In-Plane Shear Strength with Values Calculated using Equation 7.3-1 in TeR MUAP-11019.

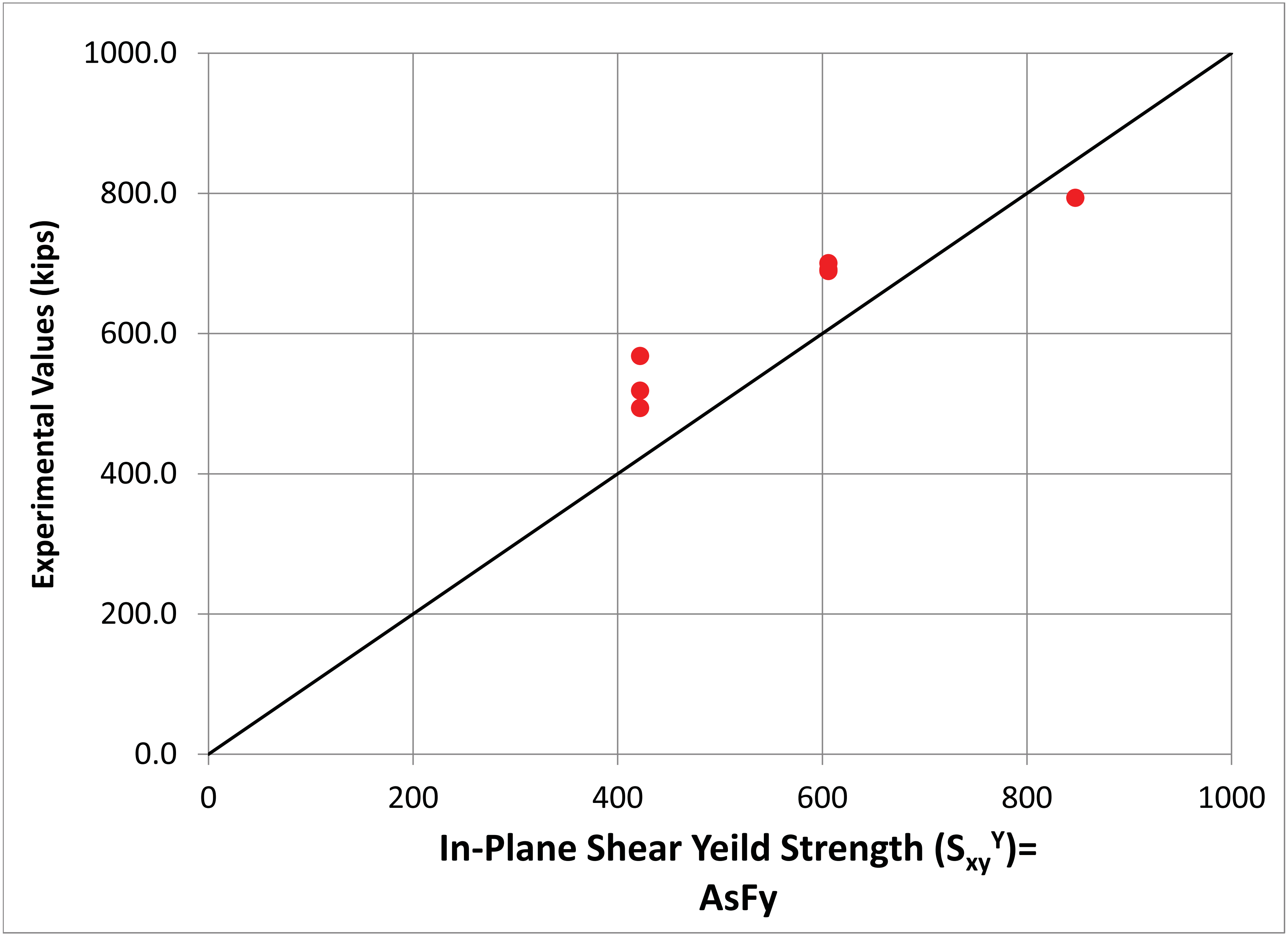

Revised Figure C-2

Table C-2 In-Plane Shear Tests of SC Walls with Flanges (References 10, 11)

Replace table with 'Revised Table C-2' attached

Revised Table C-2

Table C-2 presents the experimental database of in-plane shear (or lateral load) tests conducted on SC walls with flanges. Table C-2 includes experimental results from Funakoshi et al. 1998 (Reference 10) and Fujita et al. 1998 (Reference 11), which are listed in Table A-1. The discussion below focuses on the specimens tested by Funakoshi et al. 1998 (Reference 10).

The specimens tested by Fujita et al. (Reference 11) are not included in this discussion because those tests focused on the lateral load behavior of SC walls connected to the concrete basemat using anchor rods. Those tests focused on an SC wall-to-basemat connection, which is very different from the US-APWR SC wall-to-basemat connection.

As shown in Table C-2, the two main test parameters were steel ratio (T/t_p = the wall thickness to the steel plate thickness) and shear span ratio (H/L). The term H represents the effective wall height (the distance from the top surface of the concrete block to the center line of the loading) and the term L represents the length of the specimen in the direction of the lateral loading applied.

Specimen BS70T05 had steel ratio (T/ t_p) of 51, which corresponds to steel reinforcement ratio ($2t_p/T$) of 3.91%. It is within the range (3.0-4.0%) of the US-APWR SRRC 4 and the corresponding US-APWR Section ID is 105 (lower pressurizer walls). Specimens BS50T10, BS70T10, and BS85T10 had steel ratios (T/ t_p) of 100 and they are equivalent of steel reinforcement ratios ($2t_p/T$) of 2.0%. Specimen BS70T14 had steel ratio (T/ t_p) of 144 and its steel reinforcement ratio ($2t_p/T$) of 1.39%. The US-APWR SRRC for these specimens is SSRC-1, and corresponds to US-APWR Section ID 107 (refueling and reactor cavity walls) and 108 (north refueling cavity walls).

Specimen BS50T10 had shear span ratio (H/L) of 0.5 and specimen BS85T10 had shear span ratio of 0.85. Specimens BS70T05, BS70T10, and BS70T14 had shear span ratios (H/L) of 0.7. Specimens BS70T05, BS50T10, BS70T10, BS85T10, and BS70T14 were subjected to in-plane shear (with zero axial compression). The tests were conducted cyclically, and the envelopes of the measured cyclic in-plane shear force-displacement responses are shown in Figure C-3. The figure includes the effects of steel reinforcement ratio (t_p/T) and shear span ratio (H/L) on the in-plane shear – displacement responses.

The experimental results indicate that the initial stiffness and cracking points for shear deformation increased slightly with increase of the steel web plate thickness, t_p. However, no pronounced difference was observed since the behavior is dominated by the concrete infill. The shear yield load and maximum load increased significantly with increases in the web steel plate thickness, t_p. In addition, the stiffness decreased significantly as H/L ratio increased. The maximum load appears to be larger as H/L decreased.

Figure C-4 shows additional comparisons of the experimental results for the five test specimens with in-plane shear strength predicted by ACI 349-06 and TeR MUAP-11019 in-plane shear strength equations. The experimentally measured ultimate in-plane shear strength was divided by in-plane shear strength predicted using both equations. The ACI 349-06 equation for in-plane shear strength of reinforced concrete walls is shown in Equation C-1.

(Part 4) **Equation C-1**

$$V_N = A_s f_y + \alpha_c \cancel{\left(1 + \frac{N_u}{2000 A_g}\right)} \sqrt{f_c^{'}} A_c$$

(Part 4) Where,

- ~~N_u is axial force normal to cross-section and A_g~~ A_c is gross area of concrete section.
- For the application to flanged SC walls, flange area that intersects the web is also taken account in addition to gross area of web portion of flanged SC walls.
- b_w is web width and d is distance from extreme compression fiber to centroid of longitudinal tension reinforcement.
- α_c is the coefficient that is equal to 3.0 for wall aspect (H/L) ratio less than 1.5, and 2.0 for H/L greater than 2.0, and varies linearly between 3.0 and 2.0 for H/L ratios between 1.5 and 2.0.
- A_s is the area of the steel plates (A_s=$A_{cv}\rho_t$) of the web in addition to the steel plate area in flange that intersects the web.
- f_y is the specified yield strength for the steel plates

(Part 5f) The TeR MUAP-11019 Section ~~6.3~~ 7.3 equation is the similar to Equation ~~C-~~ C-1 with the exception that the concrete contribution to the in-plane shear strength is ignored as shown in Equation ~~C-~~ C-1.

Equation C-2 $$V_N = A_s f_y$$

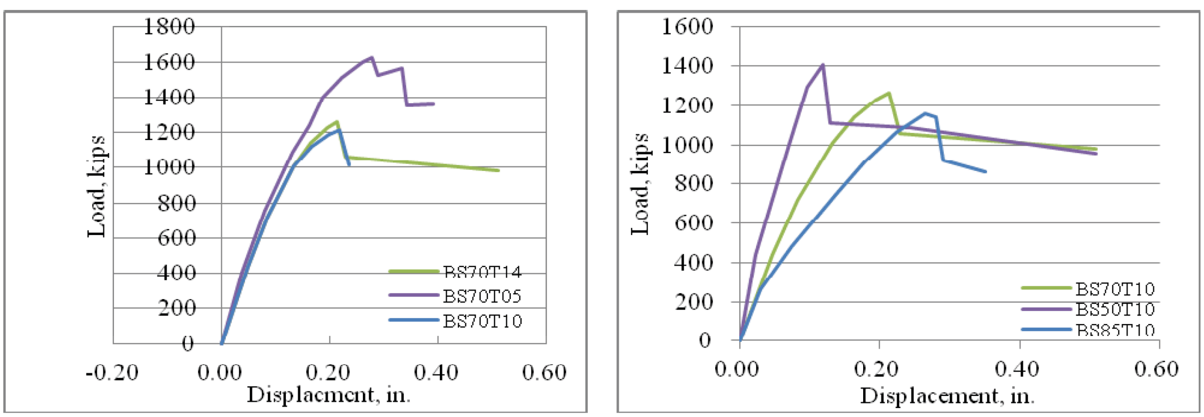

Figure C-3 In-Plane Shear Force vs. Displacement Curves: (a) Effects of reinforcement ratio, (b) Effects of aspect ratio

Axial Compression and Local Buckling Database and Comparison with Design Equation

This Appendix focuses on the experimental database of axial compression tests conducted on SC walls and the local buckling behavior of steel faceplates. The experimental database of SC wall compression tests is presented, and the test results are used to confirm the conservatism of the TeR MUAP-11019 recommended maximum plate slenderness ratio of 20.

Table D-1 presents the database of compression tests conducted on SC wall stub columns. It includes experimental results from Usami et al. (1995), Kanchi et al. (1996) and Sekimoto et al. (1996) (References 14, 15 and 16, respectively.

The main parameter in Table D-1 is the plate slenderness ratio (s/t_p), which is calculated as the largest clear spacing (s) of the steel headed stud anchors, structural shapes, or tie bars divided by the steel faceplate thickness (t_p). The specimens dimensions, loading setups, and test results are also included in the database).

As shown in Table D-1, Usami et al. (1995) (Reference 14) conducted four cyclic compression tests. Specimens NS20, NS30, NS40 and NS50 had steel reinforcement ratios ($2t_p/T$) of 3.24%, which is within the range (3%-4%) of the US-APWR SRRC 4, and corresponds to US-APWR Section ID 105 (lower pressurizer walls). However, the steel reinforcement ratio (2tp/T) is not a relevant parameter for the compression tests. The steel plate slenderness is the primary parameter of interest because it governs the local buckling of the steel faceplates and thus the axial compression strength.

NS20, NS30, NS40 and NS50

(Part 5g) Specimens ~~N20, N30, N40 and N50~~ had plate slenderness ratios (s/t_p) of 20, 30, 40 and 50, respectively. These s/t_p ratios are much larger than the s/t_p ratios (8-16) for US-APWR SC wall design for all section IDs as shown in Table A-2. TeR MUAP-11019 Section 2.2 recommends that the plate slenderness ratio (s/t_p) limit is 20. Local buckling of the steel faceplates will occur before yielding for SC walls and specimens with s/t_p ratio greater than 20. This is confirmed by the test results for all the specimens.

As shown in Table D-1, Kanchi et al. (1996) (Reference 15) conducted 11 compression tests. The compressive load was uni-directional but cyclic (load-unload-reload cyclic). The SC walls had s/t_p ratios that are greater than the s/tp ratios (8-16) for US-APWR SC wall design for all section IDs. The failure was typically due to local buckling of the steel faceplates. .

Specimens C4-20M, C4-25M, C4-30M, C4-50M and C4-30S had steel reinforcement ratios ($2t_p/T$) of 3.21%. This is within the range (3%-4%) of the US-APWR SRRC 4, and corresponds to US-APWR Section ID 105 (lower pressurizer walls). However, the steel reinforcement ratio (2tp/T) is not a relevant parameter for the compression tests. The steel plate slenderness is the primary parameter of interest because it governs the local buckling of the steel faceplates and thus the axial compression strength. Specimens C4-20M, C4-25M, C4-30M, C4-50M had 0.18 inch (4.5 mm) faceplates with plate slenderness ratios (s/t_p) of 20, 25, 30 and 50, respectively. C4-30S had 0.18 inch (4.5 mm) faceplates with s/t_p ratio of 30, but the yield stress of the steel was lower than C4-30M.

Specimens C6-20M, C6-25M, C6-30M, C6-35M, C6-40M and C6-30S had steel reinforcement ratios ($2t_p/T$) of 4.29%. This is within the range (4%-5%) of the US-APWR SRRC 5, and corresponding to US-APWR Section ID 106 (mid-height pressurizer walls). However, the steel reinforcement ratio ($2t_p/T$) is not a relevant parameter in compression tests. The steel plate

Table D-1 Compression Loading Tests (References 14, 15, 16)

Replace table with 'Revised Table D-1' attached

Response to RAI 1023-7067 Q#03.08.03-110
Attached Markup of MUAP-11005

Page 14 of 25

Revised Table D-1

The experimental results from all the tests in the experimental database have been compiled and plotted in Figure D-2. The ordinate in the plot is the normalized strain, $\varepsilon_{cr}/\varepsilon_y$, where ε_{cr} is the critical buckling strain of the steel plate from compressive tests and ε_y is the nominal yield strain of the steel plates. The abscissa is the plate slenderness ratio (s/t_p) normalized with respect to the square root of E/F_y, where E is the Young's modulus of steel. Euler's column buckling curve with effective length coefficient (K) equal to 0.7 is also plotted in the figure. It can be observed that the test data points have a trend that follows Euler's curve.

Another important observation is that there is no data that falls in the shadowed area where the normalized slenderness ratio is less than 1.0 and ε_{cr} is less than ε_y. This implies that when the normalized plate slenderness [$s/t_p \times \sqrt{F_y/E}$] ratio is less than 1.0, yielding (ε_y) occurs before local buckling (ε_{cr}). This leads to the conclusion that the slenderness ratio limit for non-compactness, i.e., yielding before local buckling in compression is given by EquationD-1.

Equation D-1 $$\frac{s}{t_p} \le 1.0\sqrt{\frac{E}{F_y}}$$

For steel faceplates with yield stress (F_y) equal to 50 ksi, Equation D-1 results in s/t_p ratio limit of 24. However, TeR MUAP-11019, Section 2.2 provides a more conservative limit of 20 for the US-APWR SC walls. Additionally, as shown in Table A-2, all the US-APWR SC walls have s/t_p ratios within the range of 8-16, much lower than the limit.

(Part 5i)

Replace figure with 'Revised Figure D-2' attached

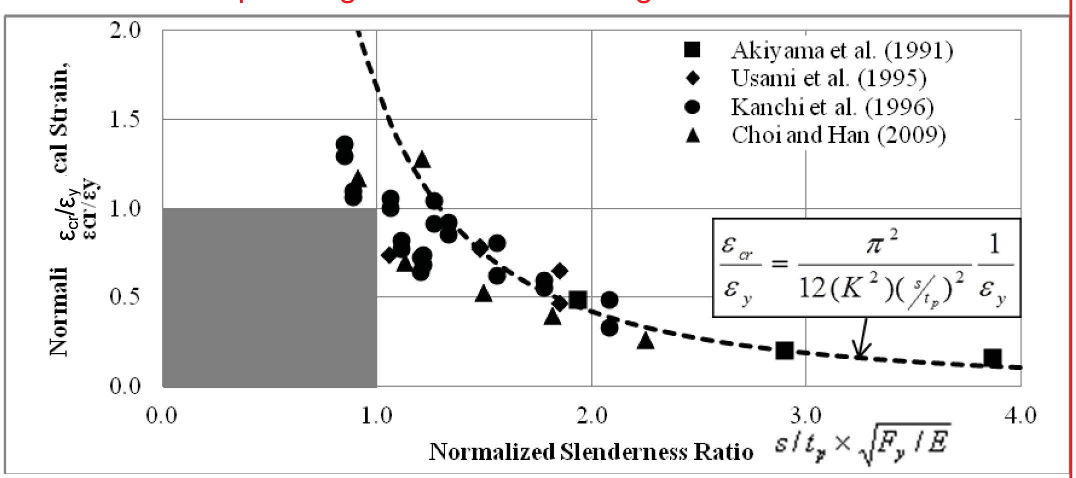

Figure D-2 Local Buckling vs. Slenderness Ratio Experimental Database

(Part 5i)

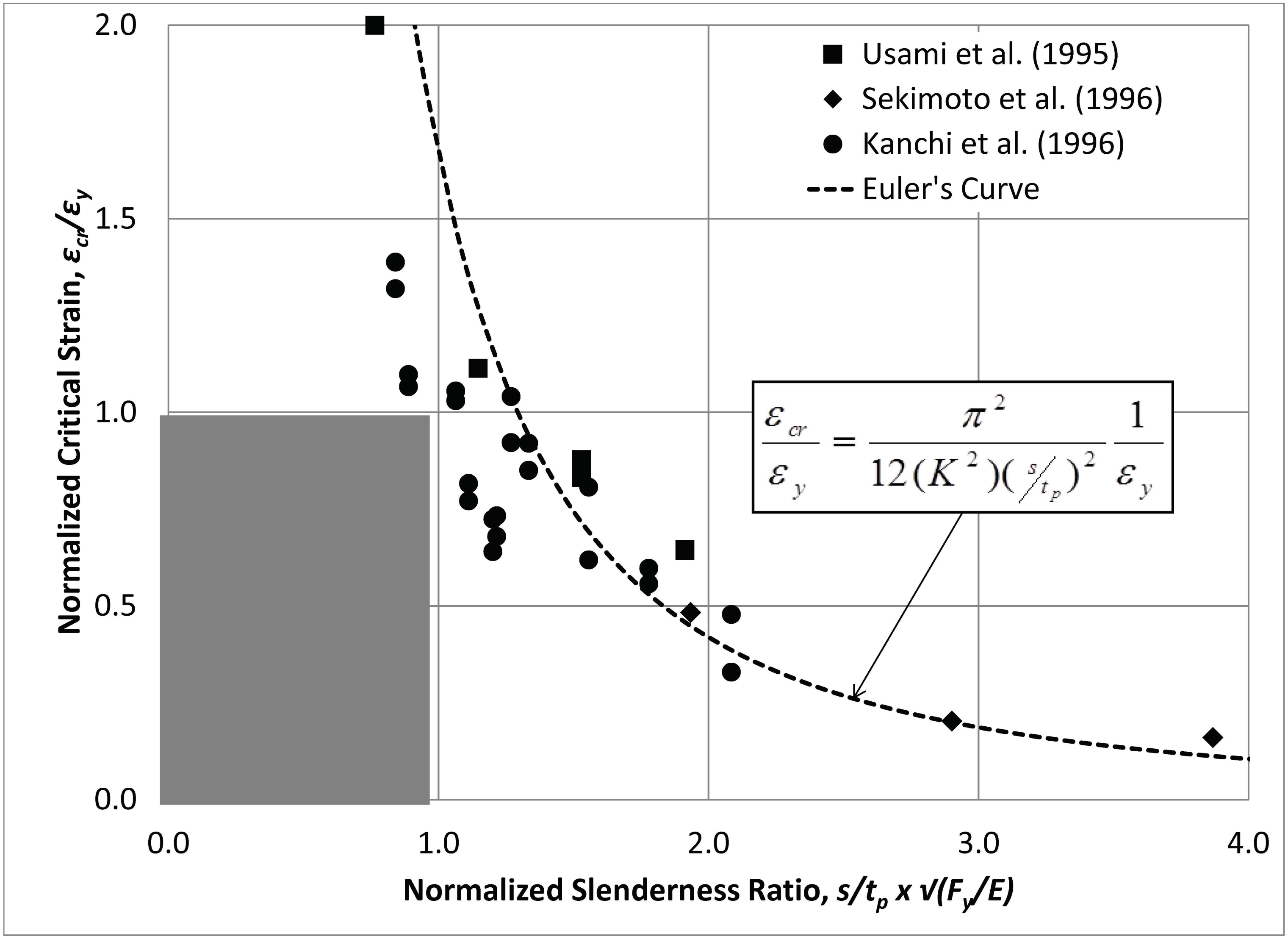

Revised Figure D-2

11. Fujita, T.; Funakoshi, A.; Akita, S.; Matsuo, I.; at el; "Experimental Study on A Concrete Filled Steel Structure Part. 14 thru Part 17 Bending Shear Tests", Summaries of Technical Papers of Annual Meeting, Architectural Institute of Japan, 1998, pp. 1121-1128

12. Kitano, T.; Akita, S., Nakazawa, M.; Fujino, Y.; Ohta, H.; Yamaguchi, T.; Nakayama, T.; "Experimental Study on a Concrete-filled Steel Structure Part 4: Shear Tests (Outline of the experimental program and the results)", Summaries of Technical Papers of Annual Meeting, Architectural Institute of Japan. B-2, pp. 1057-1058, 1997

13. Masahiko, O.; Shodo, A.; Masayuki, T.; Hirosuke, O.; Tatsuo, N.; Hironori, N.; "Experimental Study on Steel-plate-reinforced Concrete Structure Part. 41-43 Heating Tests", Summaries of Technical Papers of Annual Meeting, Architectural Institute of Japan, 2000, pp. 1127-1132

14. Usami, S.; Akiyama, H., Narikawa, M.; Hara, K.; Takeuchi, M.; and Sasaki, N.; "Study on a concrete filled steel structure for nuclear power plants (part 2). Compressive loading tests on wall members", SMiRT-13, Porto Alegre, Brazil, August, 1995

15. Kanchi, M.; et al, "Experimental Study on Concrete-filled Steel Structure: Part 2 Compressive Tests Characteristics Test (1)", Summaries of technical papers of Annual Meeting Architectural Institute of Japan. B-2, Structures II, Structural dynamics nuclear power plants 1996, 1071-1072, 1996-07-30

16. Sekimoto, H., "Experimental Study on Concrete Filled Steel Shear Wall: Part 1 Compression Test of Seismic Wall", Summaries of technical papers of Annual Meeting Architectural Institute of Japan. Structures II 1991, 1659-1660, 1991-08-01

17. Akita, S; Ozaki, M; "Earthquake-Resistant Design Recommendation for Building Using Steel Plate Reinforced Concrete Structure (Design Method of Earthquake-Resistant Wall)", Technical Report of Architectural Institute of Japan, Dec., 2001, No.14, pp123-128

18. Ozaki, M. et al, "Study on Steel Plate Reinforced Concrete Panels Subjected to Cyclic In-Plane Shear", Nuclear Engineering and Design, Volume 228, 2004

19. Varma, A.; Malushte, S.; Sener, K.; Both, P.; Coogler, K.; "Steel-Plate Composite (SC) Walls: Analysis and Design Including Thermal Effects", SMiRT 21, New Delhi, India, November 2011

(Part 2)

20. Sasaki, N., Akiyama, H., Narikawa, M., Hara, K., Takeuchi, M., and Usami, S., "Study on A Concrete Filled Steel Structure for Nuclear Power Plants Part 3 Shear and Bending Loading Tests on Wall Member," 13th International Conference on Structural Mechanics in Reactor Technology, 1995.

Reference 20

.

Study on A Concrete Filled Steel Structure for Nuclear Power Plants Part 3 Shear and Bending Loading Tests on Wall Member

Transactions of the **13th International Conference on Structural Mechanics in Reactor Technology** (SMiRT 13), Escola de Engenharia - Universidade Federal do Rio Grande do Sul, Porto Alegre, Brazil, August 13-18, 1995

Study on a concrete filled steel structure for nuclear power plants (part 3). Shear and bending loading tests on wall member

Sasaki, N.[1], Akiyama, H.[2], Narikawa, M.[3], Hara, K.[1], Takeuchi, M.[3], Usami, S.[1]
1) Kajima Corporation, Tokyo, Japan
2) University of Tokyo, Tokyo, Japan
3) Tokyo Electric Power Co., Tokyo, Japan

ABSTRACT : Bending shear tests were performed using H-section wall test specimens to determine the bending shear characteristics of an earthquake resisting wall made of a concrete filled steel structure (SC structure). The test parameters were shear span ratio, steel ratio, and axial stress. Comparison with a reinforced concrete earthquake resisting wall having the same steel ratio confirmed that the SC structure was superior in terms of both yield strength and stiffness.

1. OUTLINE OF THE TEST

1.1 Objectives

The concrete filled steel structures (SC structures) is outlined in the companion paper, Part 1. When these structures are employed in nuclear power generating plants, the SC wall member resists external lateral forces, particularly seismic forces. Therefore, in applying this type of structure, it is important to understand the characteristics of the SC wall under inplane bending shear forces. However, little research has been conducted on this problem, especially in evaluating methods of determining ultimate shear strength. Thus, bending shear loading tests similar to those for conventional reinforced concrete (RC) structures were executed on H-section wall models.

1.2 Specimens

Factors affecting the bending shear characteristics of SC structures are shear span ratio (height H / length L), steel ratio and existence of axial stress. In addition, whether or not stud bolts are incorporated to the region of the joint between the web wall and flange wall is an important factor affecting cost effectiveness and ease of construction. These factors were examined as test parameters using a total of seven test specimens. The specimens are listed in Table 1. Their cross sections were equivalent to about 1/3 to 1/2 that of a full scale wall. As it was difficult to obtain steel plates of differing thicknesses but having the same mechanical properties, the steel ratio was altered by changing the wall thickness. To obtain the shear strength of the SC structure, bending reinforcing plates were attached at the edge regions of the flange walls, so that shear failure would occur after bending yield of the flange steel plate but prior to bending failure. The configuration and dimensions of the test specimens are shown in Fig.1. Width-to-thickness ratio (stud bolt pitch/plate thickness) of the surface steel plates was chosen based on the compression test results, to prevent elastic buckling of the steel plates would not occur. A value of 33 was chosen for all specimens, the resulting stud bolt pitch being 76mm. The properties of the materials used are shown in Table 2.

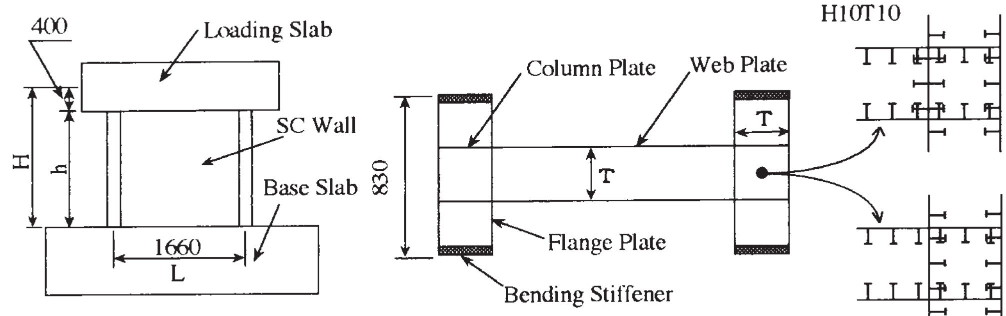

Fig.1 Test Specimen

Table 1 Summary of Specimen

Steel Ratio		Shear-Span Ratio 0.87 h=125cm	1.09 h=166cm	1.53 h=250cm
4.00 %	T=11.5cm		H10T05	
2.00 %	T=23.0cm	H07T10	H10T10 H10T10N*1 H10T10V*2	H15T10
1.33 %	T=34.5cm		H10T15	

*1: No Stud Bolts at the Connection
*2: Axial Stress of 3 MPa is Applied

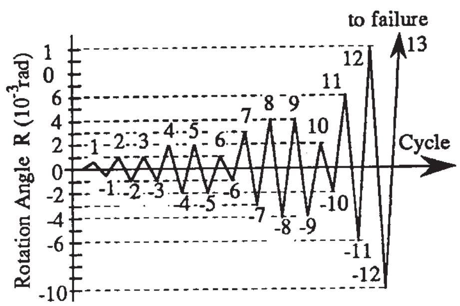

Fig.2 Loading Cycle

Table 2 Material Specification

Materials		Size	Yield Stress (MPa)	Max. Stress (MPa)	Young's Modulus (MPa)	Poisson's Ratio
Steel Plate	Web	2.3mm Thick	286	420	203000	0.28
	Column	4.5mm Thick	294	438	207000	0.29
Comcrete	I *1	——	——	29.7	20700	0.22
	II *2	——	——	32.7	23400	0.21
Stud Bolt	Web	9mm Dia × 41mm length	360	438	——	——
	Column	9mm Dia × 41mm length	357	464	——	——

*1 : Specimen H07T10, H10T05, H10T15 *2 : H10T10N, H10T10, H10T10V, H15T10

1.3 Test Method

The test specimen mat slab was fixed to the test bed using PC steel bars, and repetitive positive and negative horizontal loads were applied via the loading slab. Equal tensile and compressive loads were applied to the left and right loading slabs by hydraulic jacks. The testing apparatus is shown in Photo.1. The loading cycle is shown in Fig.2. The absolute and relative displacements were measured by LVDTs. Absolute displacements were measured against measuring frames, supported at 4 points on the mat slab. The strains in the steel plate and the concrete were measured by wire strain gages. Strain gages were also fixed in three directions to main parts, such as the web steel plate, to enable calculation of principal strain and shear strain.

2. TEST RESULTS

2.1 Observation

All test specimens demonstrated the same failure pattern, i.e., sounds of concrete cracking occurred, and the steel plates yielded, then they buckled, and finally reached maximum load. After this, depending upon the level of damage to the specimen, a further load was applied until a rotation angle of 1/40~1/25 was reached. In some specimens, cracking occurred at the foot of the flange plate on the bending tension side at close to the maximum load. At ultimate deformation, the crack split with a loud noise and a certain loss of strength occurred. Load levels at which the various events occurred are summarized in Table 2. The specimen H15T10 after loading is shown in Photo.2 (Every two intersection of the straight lines indicates stud bolt positions in the left photograph). The condition of the internal concrete of specimen H10T05 after the surface steel plates were removed can be seen in Fig.3. The following results were obtained from all specimens:

a)Buckling occurred in the region between stud bolt rows in the web plate at an angle of 45°, and also in the lower portion of the flange plate in a horizontal direction (Photo.2).

b)All steel plate buckling occurred after yielding (Table3).

c)Prominent cracks run approximately between stud bolts at an angle of 45° to the horizontal in the web concrete, and also horizontally along the flange concrete (Fig.3).

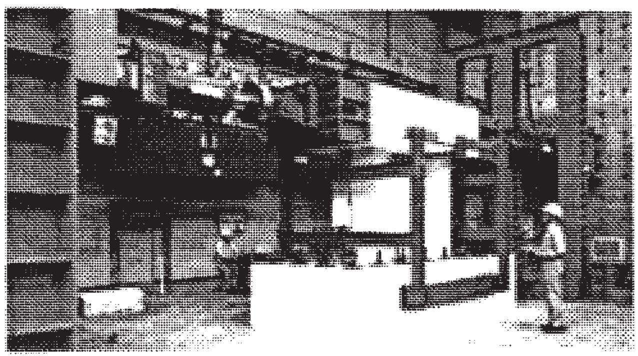

Photo.1 Testing Apparatus

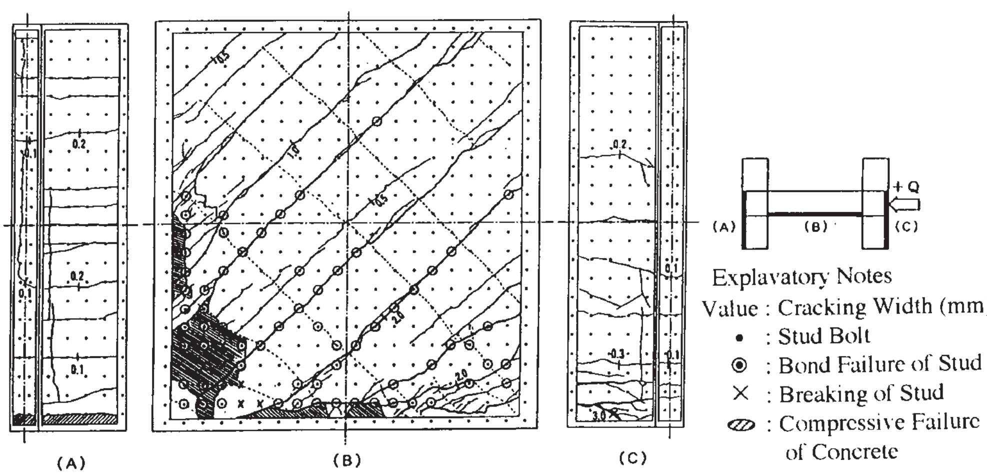

Fig.3 Concrete Surface After Loading (H10T05)

Table 3 Summary of Test Results

	Stress (MPa)					Initial Stiffness (×10 MN/cm)	Flange Plate Tensile Failure *1
	Flange Plate		Web Plate		Maximum		
	Yield	Buckling	Yield	Buckling			
H07T10	6.5	7.9	6.5	A	10.6	2.14	A
H10T05	7.1	8.8	10.1	12.5	12.6	0.83	B
H10T15	5.6	8.1	5.0	A	9.5	1.72	A
H10T10V	5.1	8.4	6.1	7.4	9.3	1.76	B
H10T10	5.7	7.2	6.0	8.5	9.4	—	B
H10T10N	8.2	9.0	6.7	8.2	11.3	1.65	N
H15T10	6.7	8.5	5.3	8.1	9.5	0.66	N

*1 : N - non occurrence, B - occurrence before Max. Load, A - occurrence After Max. Load

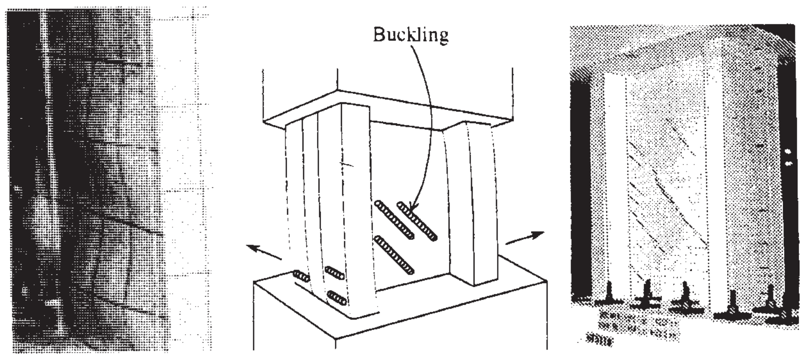

Photo.2 Specimen After Loading (H15T10)

2.2 Relation between Shear Stress and Displacement

The relations between the shear stress occurring under positive loading and the rotation angle at the top of the wall, are shown as envelope lines drawn for each parameter in Fig.4 to Fig.6. The shear stress is obtained by dividing the applied load by the effective cross sectional area shown in the same figure. The rotation angle is obtained from the absolute horizontal deformation at the top of the wall measured by the LDVT, less the outcropping deformation at the foot of the wall and divided by the internal height. Fig.7 compares the results for the test specimen with the smallest steel ratio H10T15 with those obtained in previous tests carried out on a conventional RC structure by Kanechika et al., having similar material properties and steel ratio. From these figures, the following results were obtained:

d) All test specimens were brought to the maximum load condition without sudden load drops or slippage, and a satisfactory stable load deformation relation was achieved (see Fig.4~Fig.6).

e) After the maximum load was exceeded, all specimens exhibited good ductility, keeping 70%~80% of the maximum load, although cracks occurred in flange plates of some specimens (see Fig.4~Fig.6).

f) Test specimen stiffness and strength, increased with decreasing shear span ratio and increasing steel ratio (see Fig.4, Fig.5).

g) Axial stress has little effect on stiffness, but the ultimate strength increased (see Fig.6).

h) The stud bolts in the web to flange joint region have no effect on the relation between shear stress and rotation angle (see Fig.6).

i) In terms of ductility and ultimate strength, the SC structure performs better than an equivalent RC structure (see Fig.7).

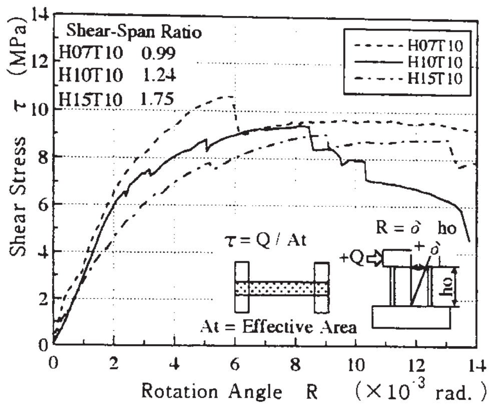

Fig.4 Shear Stress V.S. Rotation Angle for various Shear-Span Ratios

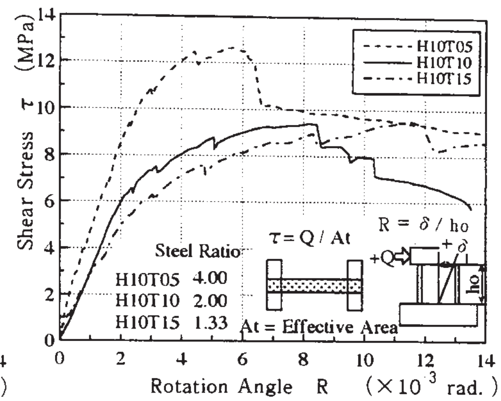

Fig.5 Shear Stress V.S. Rotation Angle for various Steel Ratios

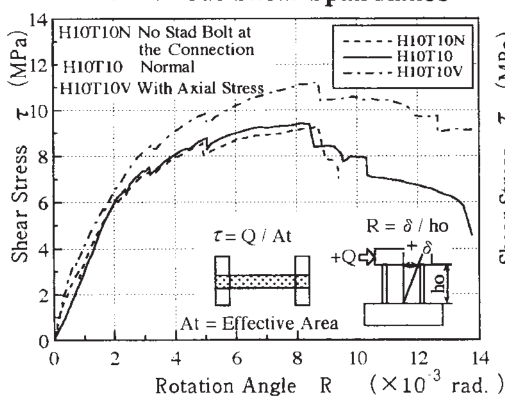

Fig.6 Shear Stress V.S. Rotation Angle for the other parameters

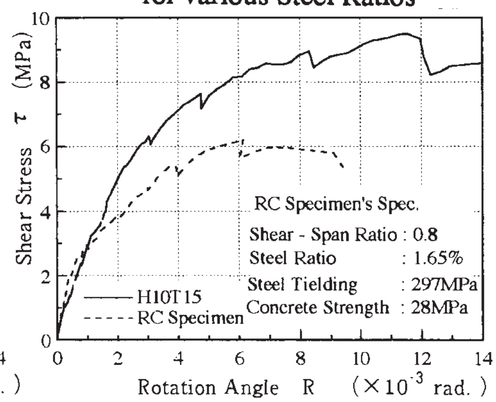

Fig.7 Shear Stress V.S. Rotation Angle for H10T15 and RC Structure

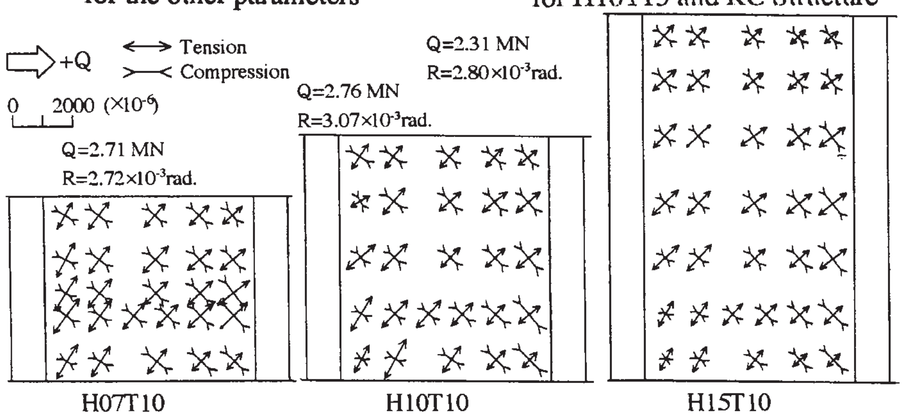

Fig.8 Principal Strain Distribution in Web Plate

2.3 Strain Distribution

The principal strain distribution and the shear strain distribution in web steel plate at the yield load level are shown in Fig.8 and Fig.9, respectively. Fig.10 shows the vertical strain distribution in the various steel plate portions at each cycle peak for specimen H10T10N. Similar results were obtained for the other test specimens. From these figures, the following results were obtained:

j)The applied load was distributed fairly uniformly over the entire surface of the web steel plate (see Fig.8).

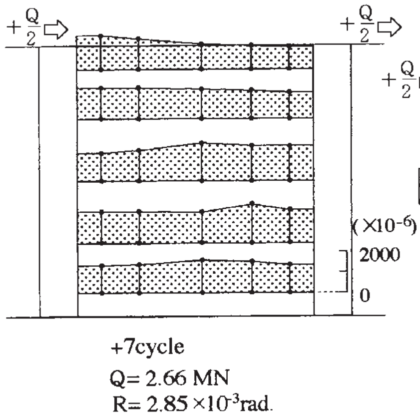

Fig.9 Shear Strain Distribution in Web Plate

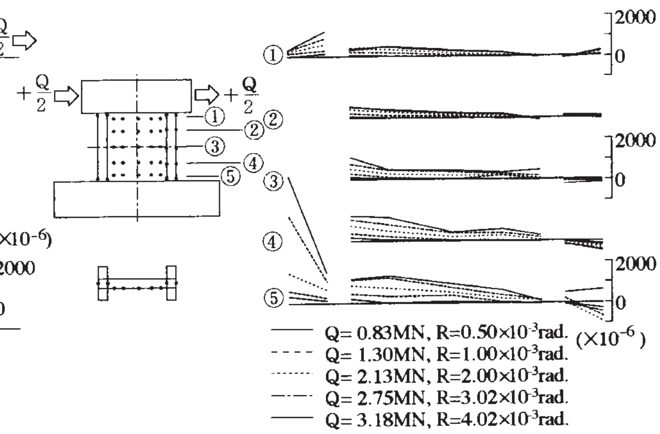

Fig.10 Vertical Strain Distribution in Steel Plate

k)Except in the region of the foot where bending moments are dominant, regardless of the shear span ratio, the direction of the principal strain acted at an angle of 45° to the horizontal (see Fig.8).

l)The shear stress was sustained fairly uniformly over the entire surface of the web steel plate (see Fig.9).

m)At the inner web portion, the vertical strain varied linearly, while at the flange portion a larger strain can be seen acting in the vertical direction. This is thought to be the effect of partial bending moment acting on the flange walls (Fig.10).

3. CONCLUSIONS

From the tests, it was confirmed that the SC structure investigated in this study exhibits superior characteristics to equivalent RC structures. The main reasons are considered to be:

i)Surface steel plate acts more effectively than steel reinforcing bars because unlike rebars it does not have directionality.

ii)The ultimate strength of the concrete is improved by the restraining effects of the steel plate.

iii)Sudden load drops caused by brittle failure of the concrete is suppressed by the steel plate.

At the present time, methods of evaluating the restoring and hysteresis characteristics with regard to shear and bending are under investigation to establish design methods for this type of structure.

REFERENCES

Fukumoto, H., Kobayashi, M., et al., 1987. Cncrete filled steel bearing walls, IABSE Vol.55: 467-472.

Kanechika, M., Satoh, S., et al., 1989. Application of high strength rebar for RC shear wall (Part1-Part7), Proc. AIJ Conf., Kumamoto:Japan

Kaneuji, A., Hara, K., et al., 1989. Feasibility study of filled steel (SC) structure for reactor building, 10th SMiRT Conf.: 67-72.

Sekimoto, H., Akiyama, H., et al., 1989. 1/10th scale model test of inner concrete structrure composed of concrete filled steel bearing wall, Proc. 10th SMiRT Conf. H73:73-78.

Usami, S., Sekimoto, H., et al., 1991. Compression and shear loading test of concrete filled steel bearing wall, Proc. 11th SMiRT Conf. H12/2: 323-328.